Hindawi
Journal of Sensors
Volume 2019, Article ID 9869682, 10 pages
https://doi.org/10.1155/2019/9869682

Research Article

Detection of Ascorbic Acid Using Green Synthesized Carbon Quantum Dots

Yuyun Wei,[1] Di Zhang,[2] Yuxin Fang,[1] Hong Wang,[1] Yangyang Liu,[1] Zhifang Xu,[1] Shenjun Wang,[1] and Yi Guo[1,3]

[1]*Research Center of Experimental Acupuncture Science, College of Acumox and Tuina, Tianjin University of Traditional Chinese Medicine, Tianjin 301617, China*
[2]*College of Pharmaceutical Engineering of Traditional Chinese Medicine, Tianjin University of Traditional Chinese Medicine, Tianjin 301617, China*
[3]*College of Chinese Medical, Tianjin University of Traditional Chinese Medicine, Tianjin 301617, China*

Correspondence should be addressed to Di Zhang; 43987073@qq.com and Yuxin Fang; meng99_2006@126.com

Received 17 September 2019; Revised 25 October 2019; Accepted 9 December 2019; Published 31 December 2019

Academic Editor: Yasuko Y. Maruo

Copyright © 2019 Yuyun Wei et al. This is an open access article distributed under the Creative Commons Attribution License, which permits unrestricted use, distribution, and reproduction in any medium, provided the original work is properly cited.

In this work, carbon quantum dots (CQDs) were synthesized by microwave irradiation and were electropolymerized on glassy carbon electrode (GCE) to establish an electrochemical sensor for the selective detection of ascorbic acid (AA). Electrochemical behaviors of the prepared sensor were investigated by cyclic voltammetry (CV), differential pulse voltammetry (DPV), and electrochemical impedance spectroscopy (EIS). Herein, two wide linear responses were obtained in ranges of 0.01-3 mM and 4-12 mM with a low detection limit of 10 μM to AA. High sensitivities (44.13 $\mu A^{-1}\,\mu M^{-1}\,cm^{-2}$, 9.66 $\mu A^{-1}\,\mu M^{-1}\,cm^{-2}$, respectively) corresponding to the linear ranges were also achieved. In addition, the electrochemical sensor exhibited good selectivity and robust anti-interference ability toward AA in the presence of dopamine (DA) and uric acid (UA). These results showed that this sensor can be used as a promising tool to detect AA in real complex systems.

1. Introduction

Ascorbic acid (vitamin C, AA) plays a crucial role as an essential nutrient and antioxidant in the human body, which exists only in food and drugs and cannot be synthesized by human beings themselves. The abnormal concentration of AA can be related to various kinds of diseases including scurvy, mental disorder, cancer, cold, AIDS, and digestive disorder [1–5]. In addition, AA has been found to participate in a lot of life processes, such as cell division, iron absorption, acceleration of collagen synthesis, melanogenesis inhibition, and metabolism [6–9]. Since AA is so important, it is of great significance to develop a rapid, sensitive analytical method for the detection of AA. Up to now, several methods have been applied for AA detection, such as chemiluminescence, fluorescence, electrochemistry, chromatography, capillary electrophoresis and colorimetry [10–15]. Of these, the electrochemical method has attracted much interest owing to its simple operation, fast response, high accuracy, high selectivity, and effectiveness.

Dopamine (DA) and uric acid (UA) coexist with AA in a biological environment [16–18]. Since the oxidation peak potential of DA and UA is close to that of AA, they often interfere with the electrochemical detection of AA. To solve this problem, researchers have used a variety of methods, among which the electrochemical sensor method [19–25] exhibits excellent anti-interference effect, which can effectively separate the peaks of AA, UA, and DA. However, there are few reports on the application of CQD modified electrode in the electrochemical detection of AA.

CQDs are a novel category of carbon nanomaterials [26] that have drawn considerable attention in recent years due to its excellent properties including low toxicity [27], nonpollution [28], high stability [29], simple preparation [30], and

extensive carbon sources. Until now, CQDs have been used in the eletrochemical detection of dopamine [31], L-cysteine [32], curcumin [33], and antipsychotics [34]; the results of these studies demonstrated that CQDs have great application prospects in the eletrochemical field. To date, methods synthesizing the CQDs have been studied extensively, such as hydrothermal [35], laser ablation [36], ultrasonic [37], microwave synthesis [38], and solvothermal [39]. Among them, the microwave method is simple, short time-consuming, environmentally friendly, and low cost.

In this paper, we have developed a sensor for AA determination based on CQDs, which were synthesized using glucose as the carbon source and polyethylene glycol-200 as the surface passivator through a one-step facile microwave approach. This fabricated CQD electrode demonstrated wider linear ranges and higher sensitivity toward AA compared to other modified electrodes based on electrochemical strategies. At the same time, the as-prepared sensor has successfully separated the oxidation peak of AA, DA, and UA. The electrochemical response of the as-prepared sensor was greatly improved and finally realized the selective detection of AA. We envision that a CQD-based sensor will become a crucial platform for determination of AA in a complex system in the future.

2. Experimental

2.1. Reagents. AA was purchased from Lianxing Biotechnology (Tianjin), polyethylene glycol-200 was bought from Beijing Solarbio Science & Technology, dopamine hydrochloride was purchased from Sigma-Aldrich, UA was obtained from Ron Chemical Reagent Company (Tianjin), glucose was obtained from Tianjin Yingda Xigui Chemical Reagent Factory, and 0.1 M phosphate buffer solution (PBS) (pH 7.0) was prepared by mixing a proper proportion of Na_2HPO_4 and NaH_2PO_4. All the other reagents were prepared with ultrapure water and directly used without further treatment.

2.2. Apparatus. All electrochemical measurements were carried out at the AMETEK PARSTAT 4000 electrochemical workstation (AMETEK Commercial Enterprise (Shanghai) Co., Ltd. Beijing Branch). All electrochemical experiments were performed with a three-electrode cell with a modified GCE as the working electrode, a platinum counter electrode (CE), and a saturated calomel electrode (SCE) as the reference electrode. A magnetic stirrer was acquired from Ronghua Instrument Manufacturing (Jiangsu, China). Field emission scanning electron microscopy (FESEM) images were obtained from Nova NanoSEM 430 (FEI, USA). High-resolution electron microscopy (HRTEM) and energy-dispersive spectrometer (EDS) micrographs were acquired by using FEI Talos F200X equipped with an energy-dispersive spectrometer analyzer. CQDs were centrifuged using a LX-400 centrifuge (Kylin-Bell Lab Instruments Co., Ltd.), microwave reactor (LG Electronics, China), and dialysis bags (Beijing Solarbio Science & Technology). All DPV measurements in this paper were performed by applying a sweep potential from -1.5 V to +1.5 V at pulse width of 0.2 s and an amplitude of 50 mV.

2.3. Synthesis of CQDs. The CQDs were synthesized by one-step microwave heating according to literature [40] with a little modification. 20 ml of polyethylene glycol-200 was added into a mixture of 6 ml of ultrapure water and 4 g of glucose under stirring condition until the solution became transparent and colorless; then, the mixed solution was placed in a microwave reactor under medium heat condition for 3 minutes. The obtained dark viscous solution was cooled down to room temperature, and then, the appropriate amount of the solution was put into a dialysis bag (cutoff Mn: 100-500 Da) for 24 hours. Then, the obtained light brown solution was centrifuged at 6000 r/min for 15 min, bottom black precipitation was removed, and the upper solution was collected and stored in the refrigerator at 4°C.

2.4. Preparation of CQD Modified GCE (CQDs/GCE). Before use, the GCE was polished to mirror with 0.05 μm alumina slurry, and then, the bare electrode was modified in CQD solution with a three-electrode system using CV under the conditions of -1~2 V, 20 cycles, at 50 mV/s. After modification, the electrode was washed with ultrapure water and dried for later use.

3. Results and Discussion

3.1. Characterization of CQDs. Morphology of CQDs was characterized by a high-resolution transmission electron microscope (HRTEM), field emission scanning electron microscope (FESEM), and energy-dispersive spectrometer (EDS). As is shown in Figure 1(a), the CQDs were found to have a quasispherical shape with a size lower than 10 nm, which is consistent with the results reported by previous literature [41, 42]. It can be seen from the inset of Figure 1(a) that the prepared CQDs possess a lattice structure with a lattice spacing of 0.14 nm, which can be attributed to the (102) diffraction plane of graphite carbon [43]. From the EDS analysis image (Figure 1(d)), the main element composition of the CQDs is C, and the peaks of Cu, O, and Si should be originated from the substrate. These results confirmed that the CQDs have been successfully synthesized. Moreover, after the CQDs were electropolymerized on the electrode surface (Figures 1(b) and 1(c)), the size of the CQDs increased (close to one hundred nanometers), which indicates that the electrochemical properties of CQDs can be improved by electropolymerization.

3.2. Electrochemical Characterization. The electrochemical properties of the bare GCE and CQDs/GCE were characterized by CV using 20 mM $Fe(CN)_6^{3-/4-}$ containing 0.1 M KCl as the electrochemical probe. As can be seen from Figure 2(a), compared with bare GCE (curve A), the peak current of CQDs/GCE (curve B) increased obviously and the interspike interval was decreased. It may be that the surface structure of CQDs can accelerate the electron transfer rate of the redox system and increase the adsorption

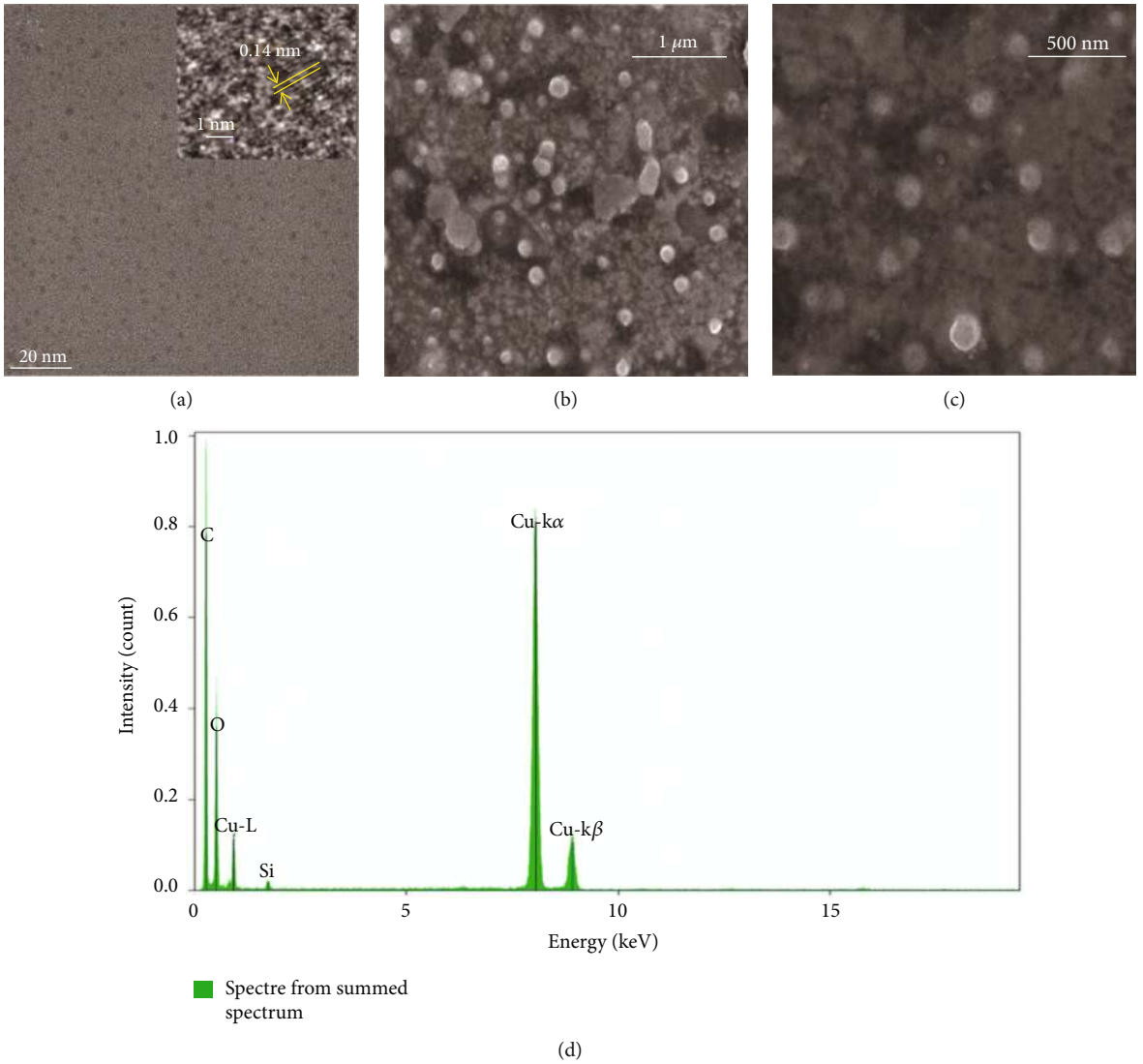

Figure 1: FRTEM (a), FESEM (b, c), and EDS analysis (d) of as-prepared CQDs.

of AA at the sensor interface. These results suggest that the prepared CQDs have good properties.

The EIS of different electrodes was measured under the conditions of 10^{-2}~10^{5} Hz, 0.24 V bias potential, and 5 V amplitude in 20 mM $Fe(CN)_6^{3-/4-}$ containing 0.1 M KCl. The direct part of the figure represents the diffusion process, and the diameter of the semicircle shows the resistance of the electron transfer. As shown in Figure 2(b), the CQDs/GCE had a smaller semicircle (curve B) than GCE (curve A), which suggested that the resistance of the modified electrode was significantly decreased, indicating that CQDs/GCE has better conductivity. The result was consistent with Figure 2(a).

DPV was also used to further evaluate the detection performance of the modified electrode in 0.1 M PBS (pH 7.0) containing 0.5 mM AA. Figure 2(c) showed that there was a broad but inapparent oxidation peak (curve A) on GCE and a narrow but obvious oxidation peak (curve B) on CQDs/GCE. The oxidation peak current of CQDs/GCE was about three times larger than that of the bare electrode, which indicated that CQDs/GCE had obvious electrocatalytic oxidation effect on AA.

3.3. Effect of Scan Rate of AA. In order to further study the reaction mechanism of AA on the as-prepared sensor surface, the effect of the scan rate on electrochemical behavior of AA was investigated. From Figure 3(a), it was observed that the catalytic current of AA on CQDs/GCE increased gradually with the increase of the scan rate, and the peak current of redox showed a good linear relationship with the scan rate in the range of 50-250 mV s^{-1} (Figure 3(b)), and the linear regression equation is demonstrated as the following, respectively: I_{pa} = -4.546-0.272 V (R^2 = 0.99), I_{pc} = 19.947 + 0.028 V (R^2 = 0.99). The results indicated that the reaction process of the modified electrode was controlled by adsorption. In addition, the oxidation peak potential and

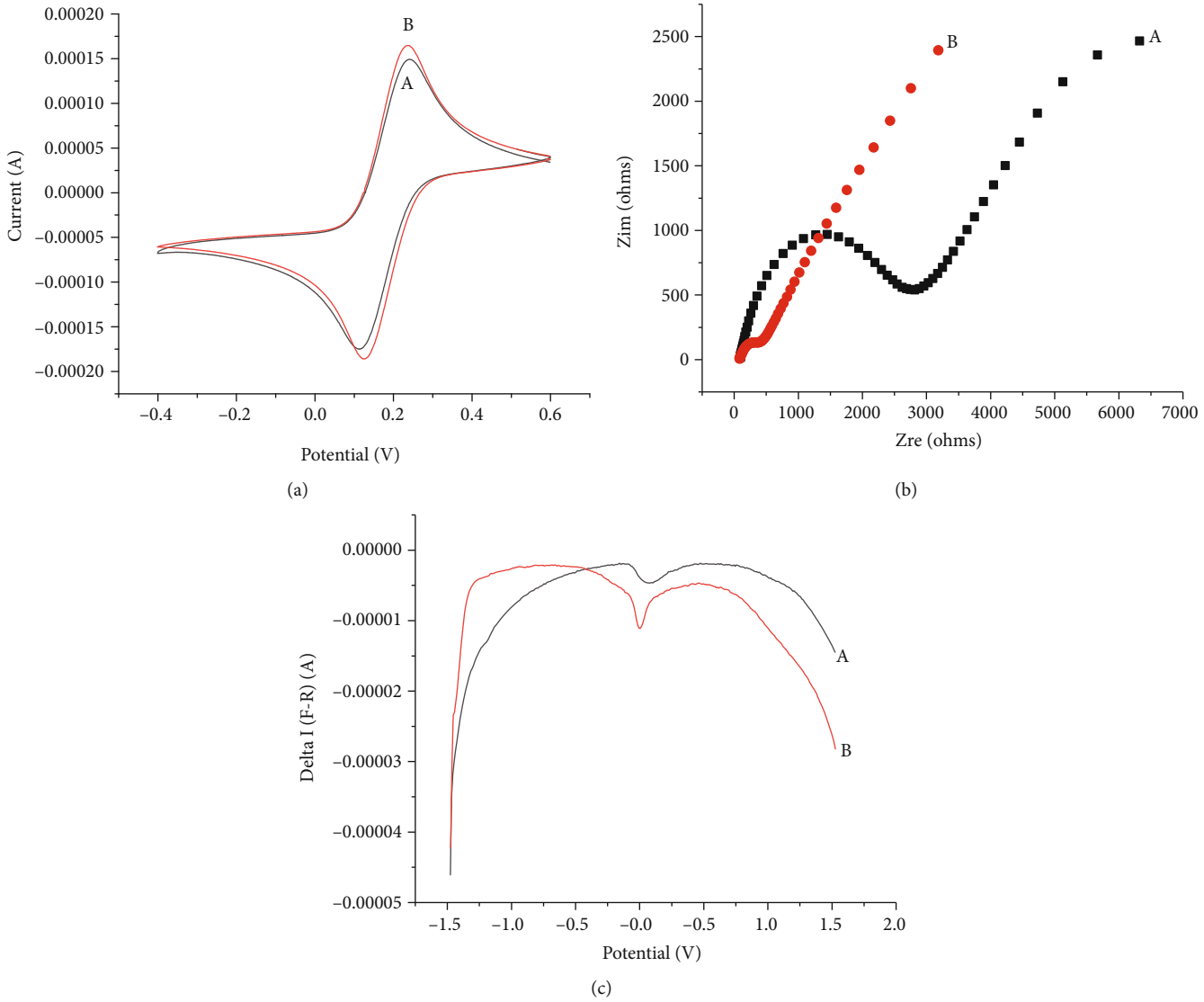

Figure 2: (a) CV grams of bare GCE (A) and CQDs/GCE (B) in 20 mM $Fe(CN)_6^{3-/4-}$ containing 0.1 M KCl. (b) Nyquist plots of bare GCE (A) and CQDs/GCE (B) in 20 mM $Fe(CN)_6^{3-/4-}$ containing 0.1 M KCl. (c) DPV response of bare GCE (A) and CQDs/GCE (B) in 0.1 M PBS (pH 7.0) containing 0.5 mM AA.

reduction peak potential almost did not change, indicating that CQDs/GCE had a good reversibility.

3.4. Electrochemical Sensing of AA on the CQDs/GCE. The electrochemical response of CQDs/GCE toward AA was studied by DPV. In the 0.1 M PBS solution, a certain amount of AA solution was added sequentially. As shown in Figure 4(a), at low concentration, the oxidation peak potential of AA remained at 0 V, and then, with the increase of AA concentration, the oxidation peak of AA existed positive transfer, which should be related to the change of the pH of the detection solution resulting from the accumulation of the oxidation product of AA. In addition, with the increase of AA concentration, the peak current of AA also increased. When AA concentration ranges from 0.01 mM to 3 mM ($R^2 = 0.995$) and from 4 mM to 12 mM ($R^2 = 0.991$), the oxidation peak current has a good linear relationship with AA concentrations (Figure 4(b)), with a detection limit of 10 μM ($S/N = 3$). Compared to many previous works based on electrochemical strategies that have been reported (Table 1), the modified electrode exhibited wider linear range and higher sensitivity. The catalytic mechanism for AA oxidation is shown in Scheme 1. The redox reaction of AA on the CQDs/GCE sensor is an electrochemical process based on two-proton and two-electron transfer, accompanied by the formation of dehydroascorbic acid.

3.5. Anti-interference of the Sensor. The anti-interference ability of the sensor to AA in the presence of DA and UA was investigated by DPV. As shown in Figure 5(a), three well-separated peaks were obtained at CQDs/GCE (curve B) while bare GCE (curve A) cannot separate the peaks of

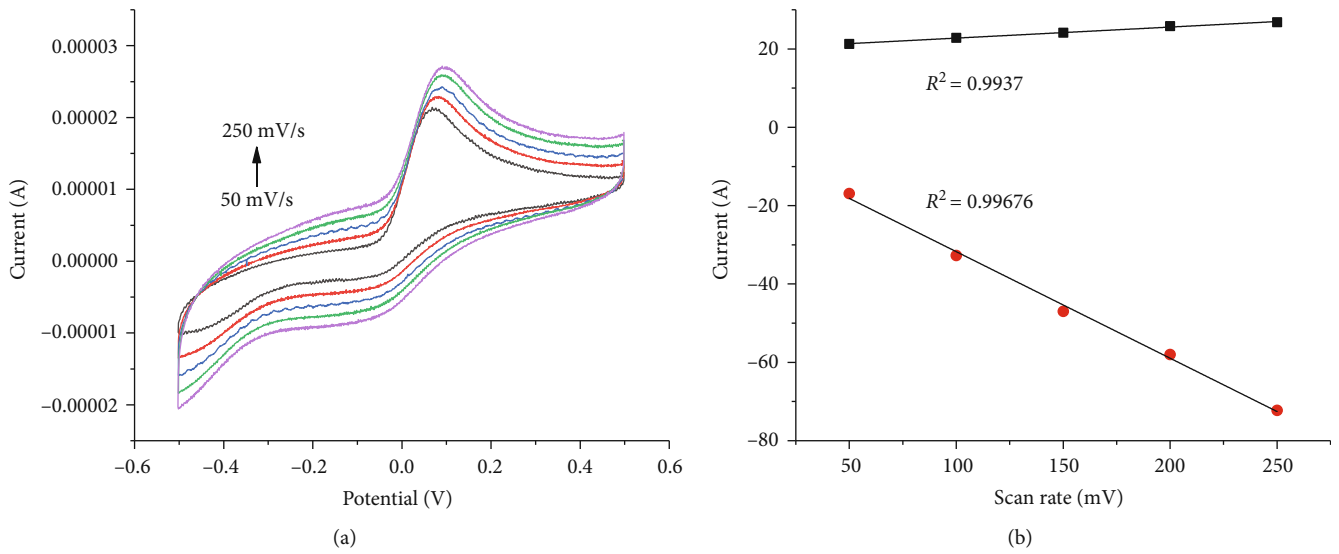

Figure 3: (a) Cyclic voltammograms of 1 mM AA on the CQDs/GCE at different scanning rates (50, 100, 150, 200, and 250 mV s^{-1}) in 0.1 M PBS (pH 7.0). (b) The effect of scanning rate on the peak current.

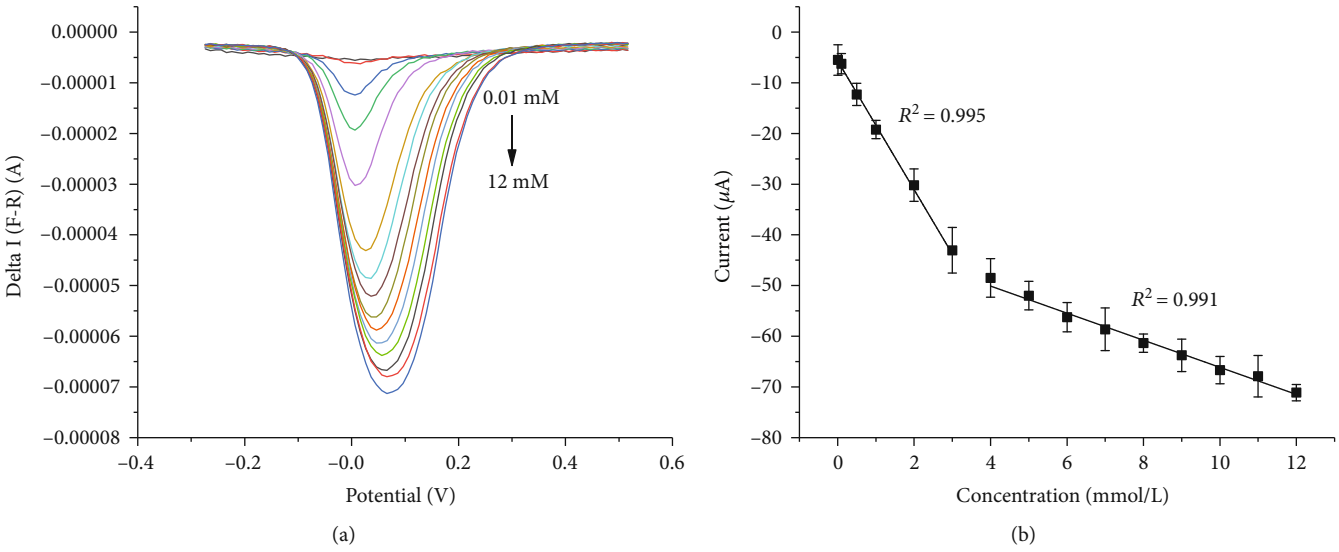

Figure 4: (a) Differential pulse voltammograms of different concentrations of AA in the ranges of 0.01~12 mM on CQDs/GCE in 0.1 M PBS (pH 7.0). (b) The linear relationship between the peak current and AA concentrations.

AA and DA. To further prove that the CQDs/GCE has good selectivity to AA, we have set control groups that only change the concentrations of AA (Figure 5(d)), DA (Figure 5(b)), and UA (Figure 5(c)) while keeping two other substances constant and changing the concentrations of AA, DA, and UA simultaneously (Figure 5(e)). These results showed that the existence of DA and UA could not interfere with the electrochemical detection of AA on the CQDs/GCE electrode. In addition, several possible interfering substances in the real sample such as Na^+, Cl^-, Mg^{2+}, SO_4^{2-}, and glucose at 100-fold concentration were also examined by chronoamperometry technique at the applied potentials of +0 V, and different substances were added every 100 seconds (Figure 5(f)), which further indicated that the prepared sensor has good selectivity for the detection of AA.

The reusability of the as-prepared sensor was investigated by six modified electrodes (Figure 6(a)) that were fabricated under the same condition in 0.1 M PBS (pH 7.0) containing 0.5 mM AA. The relative standard deviation of peak current was calculated as 3.58%, which indicated that the sensor has good reproducibility. The sensitivity of the sensor was calculated as the slope line of each electrode area (0.2826 cm^2), equal to 44.13 and 9.66 $\mu A^{-1}\,\mu M^{-1}\,cm^{-2}$,

Table 1: Comparison of electrode performance with other modified materials based on electrochemical strategies.

Electrode material	LOD (μM)	Linear range (mM)	Sensitivity ($\mu A^{-1}\ \mu M^{-1}\ cm^{-2}$)	Ref.
Q-chitosan/C	3	1×10^{-2}-5	7.6×10^{-2}	[44]
PdNi/C	5×10^{-1}	1×10^{-2}-1.8	—	[45]
Cu_2O/CuO/rGO	3×10^{-1}	1×10^{-1}-1	1.375	[46]
AgNPs-Psi	8×10^{-1}	2×10^{-2}-6×10^{-1}	1.279	[47]
Branch-trunk Ag hierarchical nanostructures	6×10^{-2}	1.7×10^{-1}-1.8	1.2	[48]
rGO-SnO_2	38.7	4×10^{-1}-1.6	1.9×10^{-2}	[49]
TOAB/YD/MWCNT	1.8×10^{-1}	1.8×10^{-1}-1.85	—	[50]
PdNWs	2×10^{-1}	2.5×10^{-1}-9×10^{-1}	—	[51]
N-CDs	3×10^{-1}	1×10^{-3}-7.5×10^{-1}	—	[52]
SN-GSEC	7.5×10^{-1}	1×10^{-3}-3	—	[53]
BN	3.77×10^{-3}	3×10^{-2}-1	—	[54]
CuNWs/GO	5×10^{-2}	1×10^{-3}-6×10^{-2}	—	[55]
MWCNT/GO/AuNR	8.5×10^{-7}	$1 \times 10^{-6} \times 10^{-5}$	7.61	[56]
GO-XDA-Mn_2O_3	6×10^{-1}	1×10^{-2}-8	6.56×10^{-1}	[21]
CuZEA/RGO	11	2×10^{-2}-2×10^{-1}	—	[57]
Zn-NiAl LDH/rGO	1.35×10^{-4}	5×10^{-4}-1.1×10^{-2}	—	[58]
CQDs	10	1×10^{-2}-3, 4-12	44.13/9.66	This work

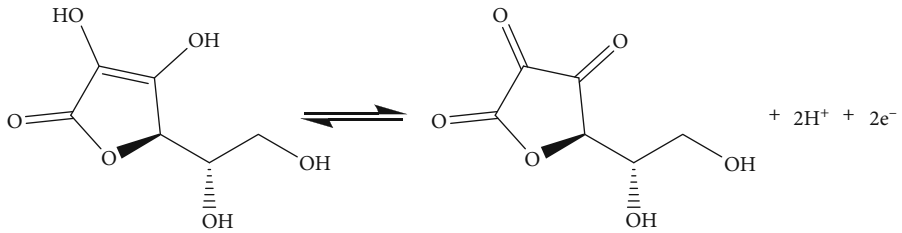

Ascorbic acid Dehydroascorbic acid

Scheme 1: Oxidation mechanism of AA on electrode surface.

respectively. As shown in Figure 6(b), the long-term durability of CQDs/GCE was measured by chronoamperometry [5, 59] under the conditions of 2000 s and 0 V; the current of the sensor decays rapidly at the beginning, which may be due to the rapid adsorption of a large number of AA on the sensor surface that makes the number of active sites reduced quickly. After that, the adsorption of AA and the release of active sites basically reached a balance, so the current of the sensor tended to be stable [19]. Since the current decay only occurs in the first few seconds, and then remains stable for a long time, it proves that the sensor has good stability.

3.6. Real Sample Analysis. To access the practical application value of the CQDs/GCE sensor, DPV was used to detect the fetal bovine serum diluted 10 times with 0.1 M PBS. The experimental results are shown in Table 2. The recoveries of AA were in the range of 99.3%-102.6%, and the relative standard deviation was lower than 3%, indicating that the sensor has important practical application of significance.

4. Conclusions

The CQDs were successfully synthesized using a microwave reactor, and the sensor based on CQDs was successfully constructed. The CQDs/GCE had two wide linear ranges, excellent sensitivity, and good stability. In particular, its outstanding anti-interference ability further indicated that CQDs are promising candidates for AA detection in real sample analysis and are expected to be used for simultaneous detection of AA, DA, and UA.

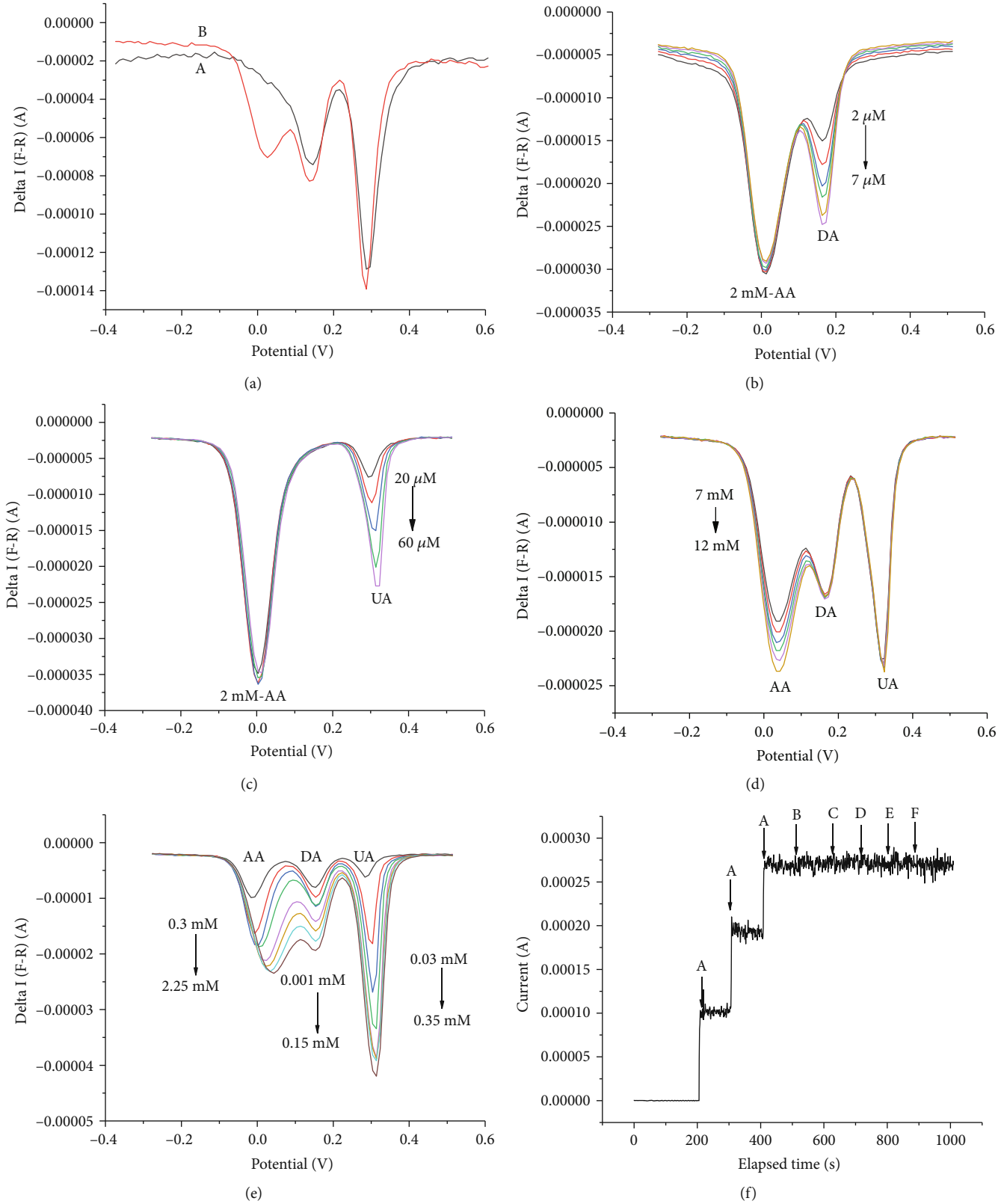

Figure 5: DPV curves of (a) 0.5 mM AA, 2 μM DA, and 0.1 mM UA on GCE (A) and CQDs/GCE (B); (b) of DA on CQDs/GCE in the presence of 2 mM AA; (c) of UA on CQDs/GCE in the presence of 2 mM AA; (d) of AA on CQDs/GCE in the presence of 4 μM DA and 20 μM UA; and (e) of AA, DA, and UA on CQDs/GCE with different concentrations. (f) Amperometric responses of CQDs/GCE upon addition of 0.5 mM AA and 50 mM other chemicals in 0.1 M PBS (pH 7.0) for 1000 s at 0 V.

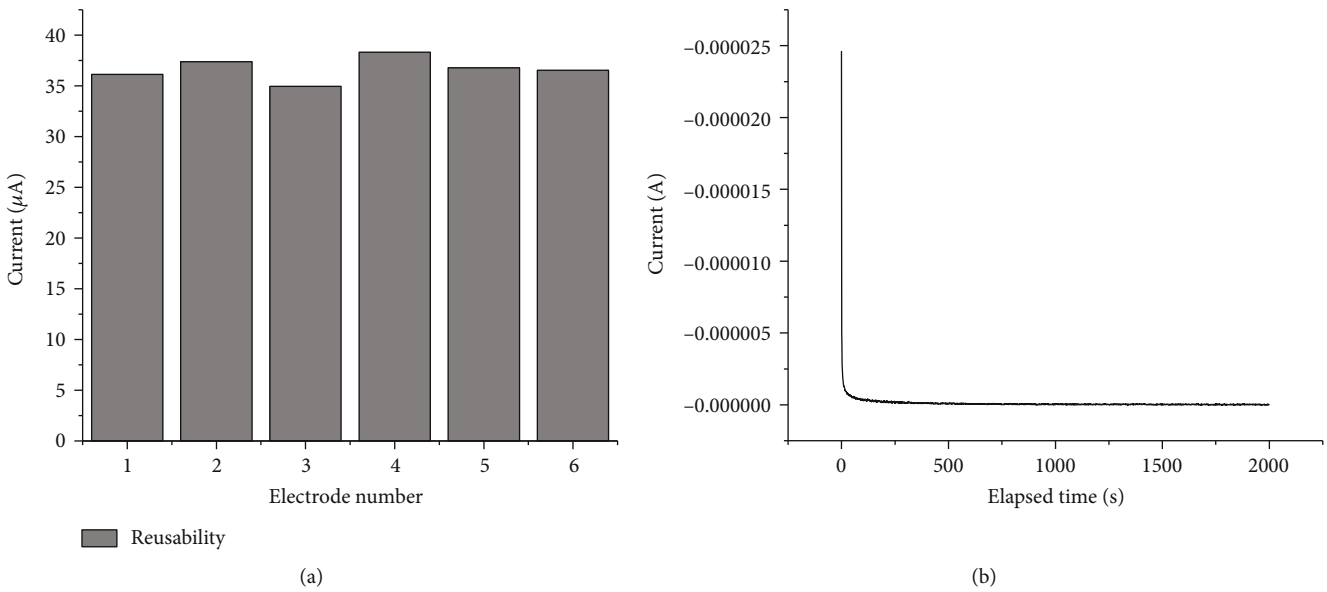

Figure 6: (a) Reusability measurement of CQDs/GCE in PBS (pH 7.0) solution containing 0.5 mM AA. (b) Stability measurement of CQDs/GCE in PBS (pH 7.0) solution containing 0.5 mM AA for 2000 s at 0 V.

Table 2: Determination of AA in fetal bovine serum sample using CQDs/GCE ($n = 6$).

Sample	Added (μM)	Found (μM)	Recovery (%)	RSD (%)
1	200	205.26	102.6	2.89
2	300	297.89	99.3	1.67
3	400	404.39	101.1	2.25

Data Availability

The generated or analysed data used to support the findings of this study are included within the article.

Conflicts of Interest

The authors declare that they have no conflicts of interest.

Acknowledgments

Financial supports from the National Natural Science Foundation of China (Grant Nos. 81973944, 81273868, and 81704146) and the National S&T Major Project (No. 2018ZX09201011) are acknowledged.

References

[1] J. Xu, J. Pan, Y. Zhang, J. Liu, L. Zeng, and X. Liu, "Ultrasensitive near-infrared fluorescence-enhanced probe for discriminative detection of GSH and Cys from different emission channels," *Sensors and Actuators B: Chemical*, vol. 238, pp. 58–65, 2017.

[2] S. A. Bsoul and G. T. Terezhalmy, "Vitamin C in health and disease," *The Journal of Contemporary Dental Practice*, vol. 5, no. 2, pp. 1–13, 2004.

[3] M. Rong, L. Lin, X. Song et al., "Fluorescence sensing of chromium (VI) and ascorbic acid using graphitic carbon nitride nanosheets as a fluorescent "switch"," *Biosensors and Bioelectronics*, vol. 68, pp. 210–217, 2015.

[4] W. Gao, Z. Liu, L. Qi, J. Lai, S. A. Kitte, and G. Xu, "Ultrasensitive glutathione detection based on lucigenin cathodic electrochemiluminescence in the presence of MnO_2 nanosheets," *Analytical Chemistry*, vol. 88, no. 15, pp. 7654–7659, 2016.

[5] D. Zhao, G. Yu, K. Tian, and C. Xu, "A highly sensitive and stable electrochemical sensor for simultaneous detection towards ascorbic acid, dopamine, and uric acid based on the hierarchical nanoporous PtTi alloy," *Biosensors & Bioelectronics*, vol. 82, pp. 119–126, 2016.

[6] H. Liu, C. Gu, C. Hou, Z. Yin, K. Fan, and M. Zhang, "Plasma-assisted synthesis of carbon fibers/ZnO core-shell hybrids on carbon fiber templates for detection of ascorbic acid and uric acid," *Sensors and Actuators B: Chemical*, vol. 224, pp. 857–862, 2016.

[7] Y. Ma, M. Zhao, B. Cai, W. Wang, Z. Ye, and J. Huang, "3D graphene foams decorated by CuO nanoflowers for ultrasensitive ascorbic acid detection," *Biosensors & Bioelectronics*, vol. 59, pp. 384–388, 2014.

[8] O. Arrigoni and M. C. De Tullio, "Ascorbic acid: much more than just an antioxidant," *Biochimica et Biophysica Acta (BBA) - General Subjects*, vol. 1569, no. 1-3, pp. 1–9, 2002.

[9] K. Kim, H. An, S. Lee, J. Seo, and J. Lim, "LB1597 palmitoyl-KVK-L-ascorbic acid inhibits melanogenesis in B16F1 cells through the down-regulation of tyrosinase and MITF," *Journal of Investigative Dermatology*, vol. 138, no. 9, article B22, 2018.

[10] I. B. Agater and R. A. Jewsbury, "Direct chemiluminescence determination of ascorbic acid using flow injection analysis," *Analytica Chimica Acta*, vol. 356, no. 2-3, pp. 289–294, 1997.

[11] H. Liu, W. Na, Z. Liu, X. Chen, and X. Su, "A novel turn-on fluorescent strategy for sensing ascorbic acid using graphene quantum dots as fluorescent probe," *Biosensors & Bioelectronics*, vol. 92, pp. 229–233, 2017.

[12] M. A. Alonso-Lomillo, O. Domínguez-Renedo, A. Saldaña-Botín, and M. J. Arcos-Martínez, "Determination of ascorbic acid in serum samples by screen-printed carbon electrodes modified with gold nanoparticles," *Talanta*, vol. 174, pp. 733–737, 2017.

[13] E. J. Oliveira and D. G. Watson, "Chromatographic techniques for the determination of putative dietary anticancer compounds in biological fluids," *Journal of Chromatography B: Biomedical Sciences and Applications*, vol. 764, no. 1-2, pp. 3–25, 2001.

[14] A. Versari, A. Mattioli, G. Paola Parpinello, and S. Galassi, "Rapid analysis of ascorbic and isoascorbic acids in fruit juice by capillary electrophoresis," *Food Control*, vol. 15, no. 5, pp. 355–358, 2004.

[15] X. Liu, X. Wang, C. Qi et al., "Sensitive colorimetric detection of ascorbic acid using Pt/CeO_2 nanocomposites as peroxidase mimics," *Applied Surface Science*, vol. 479, pp. 532–539, 2019.

[16] M. Choukairi, D. Bouchta, L. Bounab et al., "Electrochemical detection of uric acid and ascorbic acid: application in serum," *Journal of Electroanalytical Chemistry*, vol. 758, pp. 117–124, 2015.

[17] L. Zhang, J. Feng, K. C. Chou, L. Su, and X. Hou, "Simultaneously electrochemical detection of uric acid and ascorbic acid using glassy carbon electrode modified with chrysanthemum-like titanium nitride," *Journal of Electroanalytical Chemistry*, vol. 803, pp. 11–18, 2017.

[18] J. Feng, Q. Li, J. Cai, T. Yang, J. Chen, and X. Hou, "Electrochemical detection mechanism of dopamine and uric acid on titanium nitride-reduced graphene oxide composite with and without ascorbic acid," *Sensors and Actuators B: Chemical*, vol. 298, article 126872, 2019.

[19] A. Savk, B. Özdil, B. Demirkan et al., "Multiwalled carbon nanotube-based nanosensor for ultrasensitive detection of uric acid, dopamine, and ascorbic acid," *Materials Science and Engineering: C*, vol. 99, pp. 248–254, 2019.

[20] M. Liu, Y. Wen, D. Li, R. Yue, J. Xu, and H. He, "A stable sandwich-type amperometric biosensor based on poly(3,4-ethylenedioxythiophene)-single walled carbon nanotubes/ascorbate oxidase/nafion films for detection of L-ascorbic acid," *Sensors and Actuators B: Chemical*, vol. 159, no. 1, pp. 277–285, 2011.

[21] A. Ejaz and S. Jeon, "A highly stable and sensitive GO-XDA-Mn_2O_3 electrochemical sensor for simultaneous electrooxidation of paracetamol and ascorbic acid," *Electrochimica Acta*, vol. 245, pp. 742–751, 2017.

[22] V. Sharma, A. Sundaramurthy, A. Tiwari, and A. K. Sundramoorthy, "Graphene nanoplatelets-silver nanorods-polymer based *in-situ* hybrid electrode for electroanalysis of dopamine and ascorbic acid in biological samples," *Applied Surface Science*, vol. 449, pp. 558–566, 2018.

[23] H. Wang, P. H. Yang, H. H. Cai, and J. Cai, "Constructions of polyaniline nanofiber-based electrochemical sensor for specific detection of nitrite and sensitive monitoring of ascorbic acid scavenging nitrite," *Synthetic Metals*, vol. 162, no. 3-4, pp. 326–331, 2012.

[24] Z. Chen and Y. Zu, "Simultaneous detection of ascorbic acid and uric acid using a fluorosurfactant-modified platinum electrode," *Journal of Electroanalytical Chemistry*, vol. 603, no. 2, pp. 281–286, 2007.

[25] G. Darabdhara, B. Sharma, M. R. Das, R. Boukherroub, and S. Szunerits, "Cu-Ag bimetallic nanoparticles on reduced graphene oxide nanosheets as peroxidase mimic for glucose and ascorbic acid detection," *Sensors and Actuators B: Chemical*, vol. 238, pp. 842–851, 2017.

[26] B. B. Chen, M. L. Liu, C. M. Li, and C. Z. Huang, "Fluorescent carbon dots functionalization," *Advances in Colloid and Interface Science*, vol. 270, pp. 165–190, 2019.

[27] Y. Yan, J. H. Liu, R. S. Li, Y. F. Li, C. Z. Huang, and S. J. Zhen, "Carbon dots synthesized at room temperature for detection of tetracycline hydrochloride," *Analytica Chimica Acta*, vol. 1063, pp. 144–151, 2019.

[28] Y. Ye, D. Yang, and H. Chen, "A green and effective corrosion inhibitor of functionalized carbon dots," *Journal of Materials Science & Technology*, vol. 35, no. 10, pp. 2243–2253, 2019.

[29] S. Zhang, L. Zhang, L. Huang et al., "Study on the fluorescence properties of carbon dots prepared via combustion process," *Journal of Luminescence*, vol. 206, pp. 608–612, 2019.

[30] S. Sagbas and N. Sahiner, "Carbon dots: preparation, properties, and application," in *Nanocarbon and its composites*, A. Khan, Ed., pp. 651–676, Woodhead Publishing, 2019.

[31] S. Hu, Q. Huang, Y. Lin et al., "Reduced graphene oxide-carbon dots composite as an enhanced material for electrochemical determination of dopamine," *Electrochimica Acta*, vol. 130, pp. 805–809, 2014.

[32] N. Amini, M. Shamsipur, M. B. Gholivand, and A. Barati, "A glassy carbon electrode modified with carbon quantum dots and polyalizarin yellow R dyes for enhanced electrocatalytic oxidation and nanomolar detection of L-cysteine," *Microchemical Journal*, vol. 131, pp. 9–14, 2017.

[33] R. M. Shereema, T. P. Rao, V. B. Sameer Kumar et al., "Individual and simultaneous electrochemical determination of metanil yellow and curcumin on carbon quantum dots based glassy carbon electrode," *Materials Science and Engineering: C*, vol. 93, pp. 21–27, 2018.

[34] G. Muthusankar, A. Sangili, S. M. Chen et al., "In situ assembly of sulfur-doped carbon quantum dots surrounded iron(III) oxide nanocomposite; a novel electrocatalyst for highly sensitive detection of antipsychotic drug olanzapine," *Journal of Molecular Liquids*, vol. 268, pp. 471–480, 2018.

[35] Y. Li, F. Liu, J. Cai et al., "Nitrogen and sulfur co-doped carbon dots synthesis via one step hydrothermal carbonization of green alga and their multifunctional applications," *Microchemical Journal*, vol. 147, pp. 1038–1047, 2019.

[36] H. Gonçalves, P. A. S. Jorge, J. R. A. Fernandes, and J. C. G. Esteves da Silva, "Hg(II) sensing based on functionalized carbon dots obtained by direct laser ablation," *Sensors and Actuators B: Chemical*, vol. 145, no. 2, pp. 702–707, 2010.

[37] H. Huang, Y. Cui, M. Liu et al., "A one-step ultrasonic irradiation assisted strategy for the preparation of polymer-functionalized carbon quantum dots and their biological imaging," *Journal of Colloid and Interface Science*, vol. 532, pp. 767–773, 2018.

[38] Y. Jiang, B. Wang, F. Meng, Y. Cheng, and C. Zhu, "Microwave-assisted preparation of N-doped carbon dots as a biosensor for electrochemical dopamine detection," *Journal of Colloid and Interface Science*, vol. 452, pp. 199–202, 2015.

[39] M. Li, C. Yu, C. Hu et al., "Solvothermal conversion of coal into nitrogen-doped carbon dots with singlet oxygen generation and high quantum yield," *Chemical Engineering Journal*, vol. 320, pp. 570–575, 2017.

[40] H. Zhu, X. Wang, Y. Li, Z. Wang, F. Yang, and X. Yang, "Microwave synthesis of fluorescent carbon nanoparticles with

electrochemiluminescence properties," *Chemical Communications*, vol. 34, no. 34, pp. 5118–5120, 2009.

[41] B. Yao, H. Huang, Y. Liu, and Z. Kang, "Carbon dots: a small conundrum," *Trends in Chemistry*, vol. 1, no. 2, pp. 235–246, 2019.

[42] N. Pourreza and M. Ghomi, "Green synthesized carbon quantum dots from Prosopis juliflora leaves as a dual off-on fluorescence probe for sensing mercury (II) and chemet drug," *Materials Science and Engineering: C*, vol. 98, pp. 887–896, 2019.

[43] L. Yang, N. Huang, Q. Lu et al., "A quadruplet electrochemical platform for ultrasensitive and simultaneous detection of ascorbic acid, dopamine, uric acid and acetaminophen based on a ferrocene derivative functional Au NPs/carbon dots nanocomposite and graphene," *Analytica Chimica Acta*, vol. 903, pp. 69–80, 2016.

[44] H. D. Jirimali, R. K. Nagarale, D. Saravanakumar, J. M. Lee, and W. Shin, "Hydroquinone modified chitosan/carbon film electrode for the selective detection of ascorbic acid," *Carbohydrate Polymers*, vol. 92, no. 1, pp. 641–644, 2013.

[45] X. Zhang, Y. Cao, S. Yu, F. Yang, and P. Xi, "An electrochemical biosensor for ascorbic acid based on carbon-supported PdNinanoparticles," *Biosensors and Bioelectronics*, vol. 44, pp. 183–190, 2013.

[46] B. Wang, J. He, F. Liu, and L. Ding, "Rapid synthesis of Cu_2O/CuO/rGO with enhanced sensitivity for ascorbic acid biosensing," *Journal of Alloys and Compounds*, vol. 693, pp. 902–908, 2017.

[47] F. A. Harraz, M. Faisal, A. E. Al-Salami et al., "Silver nanoparticles decorated stain-etched mesoporous silicon for sensitive, selective detection of ascorbic acid," *Materials Letters*, vol. 234, pp. 96–100, 2019.

[48] Y. Zhang, P. Liu, S. Xie et al., "A novel electrochemical ascorbic acid sensor based on branch-trunk Ag hierarchical nanostructures," *Journal of Electroanalytical Chemistry*, vol. 818, pp. 250–256, 2018.

[49] R. Sha and S. Badhulika, "Facile green synthesis of reduced graphene oxide/tin oxide composite for highly selective and ultra-sensitive detection of ascorbic acid," *Journal of Electroanalytical Chemistry*, vol. 816, pp. 30–37, 2018.

[50] D. Huang, X. Li, M. Chen et al., "An electrochemical sensor based on a porphyrin dye-functionalized multi-walled carbon nanotubes hybrid for the sensitive determination of ascorbic acid," *Journal of Electroanalytical Chemistry*, vol. 841, pp. 101–106, 2019.

[51] D. Wen, S. Guo, S. Dong, and E. Wang, "Ultrathin Pd nanowire as a highly active electrode material for sensitive and selective detection of ascorbic acid," *Biosensors and Bioelectronics*, vol. 26, no. 3, pp. 1056–1061, 2010.

[52] Y. Zhang, X. Fang, H. Zhao, and Z. Li, "A highly sensitive and selective detection of Cr(VI) and ascorbic acid based on nitrogen-doped carbon dots," *Talanta*, vol. 181, pp. 318–325, 2018.

[53] L. Huang, Y. Cao, and D. Diao, "Surface N-doped graphene sheets induced high electrocatalytic activity for selective ascorbic acid sensing," *Sensors and Actuators B: Chemical*, vol. 283, pp. 556–562, 2019.

[54] Q. Li, C. Huo, K. Yi, L. Zhou, L. Su, and X. Hou, "Preparation of flake hexagonal BN and its application in electrochemical detection of ascorbic acid, dopamine and uric acid," *Sensors and Actuators B: Chemical*, vol. 260, pp. 346–356, 2018.

[55] W. Hao, Y. Zhang, J. Fan et al., "Copper nanowires modified with graphene oxide nanosheets for simultaneous voltammetric determination of ascorbic acid, dopamine and acetaminophen," *Molecules*, vol. 24, no. 12, article 2320, 2019.

[56] Y. Zhao, J. Qin, H. Xu et al., "Gold nanorods decorated with graphene oxide and multi-walled carbon nanotubes for trace level voltammetric determination of ascorbic acid," *Microchimica Acta*, vol. 186, no. 1, p. 17, 2018.

[57] P. He, W. Wang, L. du, F. Dong, Y. Deng, and T. Zhang, "Zeolite A functionalized with copper nanoparticles and graphene oxide for simultaneous electrochemical determination of dopamine and ascorbic acid," *Analytica Chimica Acta*, vol. 739, pp. 25–30, 2012.

[58] M. Asif, A. Aziz, H. Wang et al., "Superlattice stacking by hybridizing layered double hydroxide nanosheets with layers of reduced graphene oxide for electrochemical simultaneous determination of dopamine, uric acid and ascorbic acid," *Microchimica Acta*, vol. 186, no. 2, p. 61, 2019.

[59] H. Yang, J. Zhao, M. Qiu et al., "Hierarchical bi-continuous Pt decorated nanoporous Au-Sn alloy on carbon fiber paper for ascorbic acid, dopamine and uric acid simultaneous sensing," *Biosensors and Bioelectronics*, vol. 124-125, pp. 191–198, 2019.

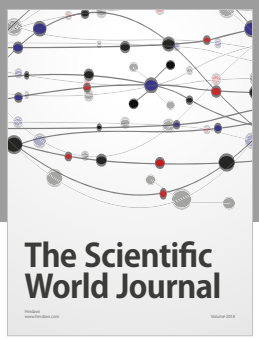

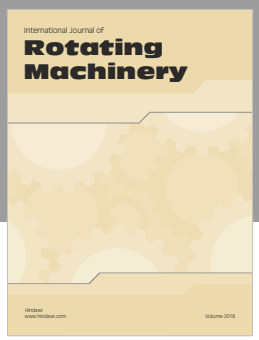

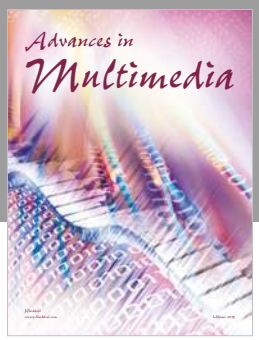

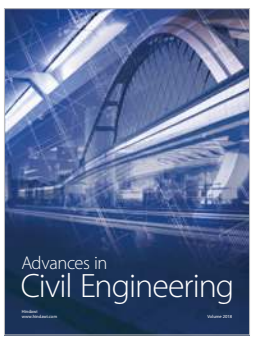

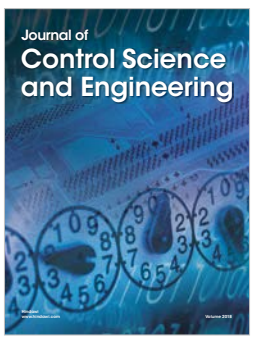

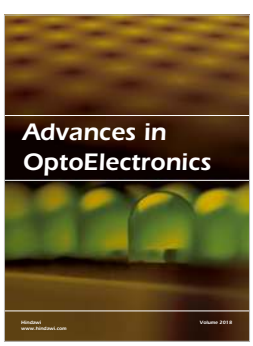

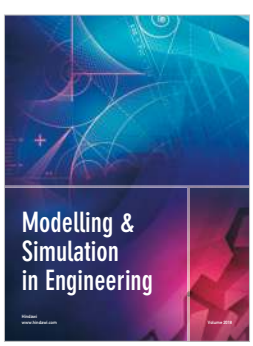

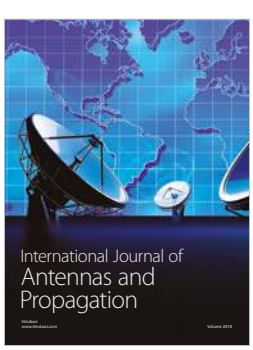

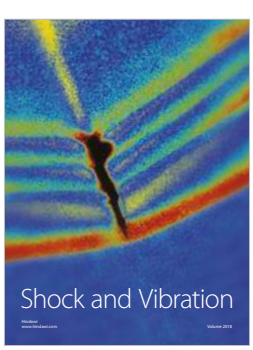

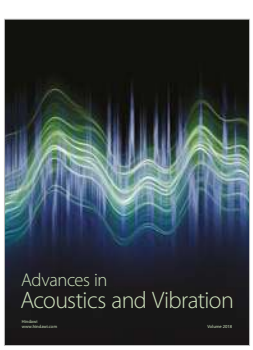

Hindawi

Submit your manuscripts at
www.hindawi.com